Nuclear Engineering and Technology 54 (2022) 2871–2876

Contents lists available at ScienceDirect

Nuclear Engineering and Technology

journal homepage: www.elsevier.com/locate/net

Original Article

Radiation effect on the polymer-based capacitive relative humidity sensors

I.V. Shchemerov [a, *], S.A. Legotin [a], P.B. Lagov [a, b], Y.S. Pavlov [b], K.I. Tapero [a, c], A.S. Petrov [c], A.V. Sidelev [c], V.S. Stolbunov [d], T.V. Kulevoy [d], M.E. Letovaltseva [e], V.N. Murashev [a], M.P. Konovalov [a], V.N. Kirilov [a]

[a] National University of Science and Technology "MISiS", Leninskyi p-t 4, Moscow, 119049, Russia
[b] A.N. Frumkin Institute of Physical Chemistry and Electrochemistry Russian Academy of Sciences, Leninskyi p-t 31, Moscow, 119071, Russia
[c] Research Institute of Scientific Instruments, Industrial Zone "Turaevo" 8, Lytkarino, 140080, Russia
[d] Institute of Theoretical and Experimental Physics, Bolshaya Cheremushinskaya 27, Moscow, 117218, Russia
[e] Russian Technological University MIREA, Vernadskogo pr-t 78, Moscow, 119454, Russia

ARTICLE INFO

Article history:
Received 22 July 2021
Received in revised form
3 February 2022
Accepted 27 February 2022
Available online 7 March 2022

Keywords:
Relative humidity
Sensor irradiation
Sensitivity degradation under irradiation

ABSTRACT

The sensitivity of polymer-based capacitive relative humidity (RH) sensors after irradiation with neutrons, electrons and protons was measured. Degradation consists of the decreasing of the upper RH limit that can be measured. At the same time, low RH-level sensitivity is almost stable. After 30 krad of absorption dose, RH cut off is equal to 85% of max value, after 60 krad−40%. Degradation reduces after annealing which indicates high radiation sensitivity of the internal circuit in comparison to RH-sensing polymer film.

1. Introduction

The LHCb detector [1] is designed for precise measurements of charge-parity symmetry violation observables and rare b and c hadron decays, exploiting the very large heavy quark production at CERN's Large Hadron Collider. The LHCb detector is a single-arm forward spectrometer covering the pseudorapidity range $2 < \eta < 5$ [1,2]. The detector includes a high-precision tracking system consisting of a silicon micro-strip vertex detector called Upstream Tracker (UT). UT employs silicon micro-strip detectors located upstream of a dipole magnet and surrounded the pp interaction region [3].

In order to ensure adequate environment conditions, the UT detector should be isolated from its surroundings. The ambient temperature in the LHCb cavern is ~20 °C, but silicon sensors will be cooled down to −5 °C using CO_2 cooling system. UT box should be gas tight to avoid moisture condensation on the detector and the beam pipe. The detector will be continuously blown with dry N_2, so humidity measurements *in situ* are needed. It can be dangerous to measure relative humidity (RH) level far from the cooling zone. Magnus equation [4] predicts that dew point will be higher than −5 °C and water will condense on the silicon detectors if RH in the nitrogen flow at 20 °C rises to 15% (see Fig. 1). Also, silicon detectors work at high electric field and increasing RH from 10 to 30% reduces the dielectric strength of air by 5% [5]. It is therefore necessary to measure humidity in the UT box directly to prevent critical damage of silicon detectors and readout chips.

A lot of humidity sensors including commercially available are used in scientific laboratories. Most of them could be irrelevant for high energy experiments due to high radiation level. The expected radiation dose after 1 year of LHCb operation (50 fb^{-1} of total integrated luminosity) is ~10^4 krad near the beam pipe and ~10 krad in the corners of the UT box [6]. This factor significantly limits the construction of the humidity sensor. In Ref. [7] the optical RH sensor based on fibre Bragg gratings was described. This RH sensor can be irradiated up to 9000 krad but its complexity and high cost do not allow using it in a lot of different points near the detector. The same idea described in Ref. [8]: fiber-optics humidity sensor is based on humidity-sensing material whose optical characteristics change with humidity.

* Corresponding author.
E-mail address: ivan.shchemerov@cern.ch (I.V. Shchemerov).

https://doi.org/10.1016/j.net.2022.02.027

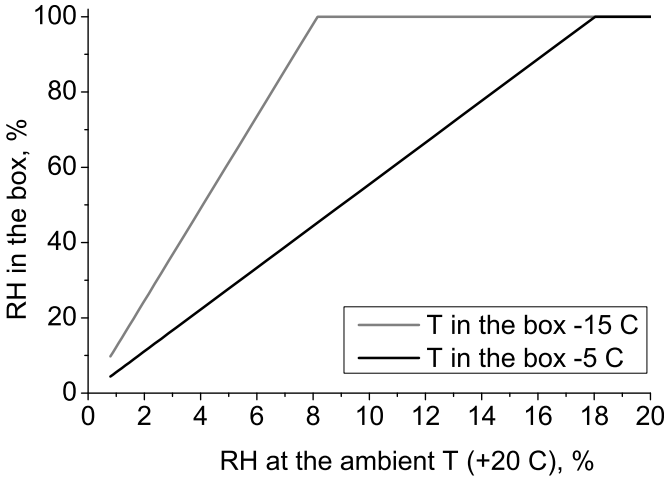

Fig. 1. Increasing of RH when gas is cooled from ambient to lower temperatures in the box.

At the same time, capacitive sensors based on vapour-sensitive polymers also have fine radiation hardness. Capacitive sensors can be divided into three types:

1. The simplest capacitor-like structure, based on vapour-sensitive polymer film (Honeywell HIH-1000, TE connectivity HS1101LF etc.). This type of sensor consists of thin polymer film that changes its capacity with humidity (see very detailed review by A. Kapic in Ref. [9]). The capacitance of those sensors can be measured by the bridge method or by a simple LCR-meter. In Ref. [10] the proton irradiation tests showed good radiation tolerance of polymer-based RH sensors. Output signal correlated with capacitance slightly increases with fluence: $5.6 \cdot 10^{-15}$% RH/(protons·cm^{-2}).
2. Simple device based on the polymer capacitor and internal silicon-based capacitance-to-voltage conversion circuit (Honeywell HIH-4000, TE connectivity HM1500LF etc.). Specific implementation for each device can be different. In most cases, the converter compares the current relaxation time by the polymer structure and reference capacitor. Description of the circuit can be found elsewhere (e.g. Ref. [11]). The most radiation-sensitive parts of these detectors are the internal 555 timer and amplifier.
3. Complex detector that includes polymer sensor, RC-circuits, amplifier, calibration circuit, analog-to-digital converter (ADC) with I2C-bus (Honeywell HIH-8000, Texas instruments HDC3020, Waveshare DHT11, Sensirion SHT40 etc.). The radiation hardness of commonly used ADC-based systems is very weak [12,13]. But in the low-radiation environment it is much more convenient to use this type of humidity detector.

The most vulnerable to radiation parts of this type of sensor is the internal circuit: silicon-based AC voltage generator, rectifier, amplifier and transmitter. The simplest structures should be more stable. At the same time making precise measurements on the devices without any internal electronics is difficult because of small changes in capacitance (typically 0.65 pF/%RH with 330 pF background). Radiation-induced degradation of the internal electronic circuit still needs to be assessed.

This work investigates the radiation effect on the polymer-based humidity sensor with a simple internal circuit and its suitability for humidity monitoring in High Energy Physics experiments.

2. Samples and methodology

The object of study is the commercial RH sensor Honeywell HIH-4000 based on humidity-sensitive thin polymer film on the silicon substrate. The capacitance of the polymer film depends on humidity. The internal circuit converts capacitance to voltage, the output signal is the linear function of RH level. The structure of the sensor is shown on Fig. 2. The thickness of silicon substrate is 0.5 mm, thickness of the aluminium case is 2 mm. The set of 6 humidity sensors HIH-4000 (1 for reference) was initially measured. The measuring circuit is shown on Fig. 3. Two samples (irradiated and reference) was connected to the same DC source (common GND and V_{in} is +5V). The measurements were provided in a closed plastic box. When water was poured into the box (or the box was blown out by dry air) the humidity level changed. RH signal was calculated as a linear function of output voltage (V_{out}) described in Ref. [14]:

$$RH = (V_{out}\text{-}a)/b \quad (1)$$

where, a ≈ 0.8 V, b ≈ 32 mV/%RH, exact coefficients depends on the structure. The measurements were provided in different environments and results by different devices were compared. The difference in output signals for all samples before irradiation does not exceed 3% RH. Accuracy of RH sensor (from datasheet [14]) is ±3.5% RH, accuracy of power source and voltage measuring system is ±1% and ±0.2% respectively. Further, we will assume that sample is still working if the difference between RH measured by irradiated and non-irradiated samples does not exceed the sum of relative and absolute errors almost everywhere. This is an acceptable assumption in our conditions, but in other cases, more precise measurements should be provided. The accuracy of capacitive RH sensors drops dramatically when humidity is out of range 5%–95% RH, so our conclusions will only apply to this range.

Devices were irradiated by neutrons, protons and electrons. The damage produced by irradiation can be classified into two categories: atomic displacement and charge deposition by ionization. Total ionizing dose (TID) and Displacement damage dose (DDD) was calculated for the Si-based internal circuit.

Measured samples and fluences:

Dev0: Reference.

Dev1: 1 MeV $1.5 \cdot 10^{12}$ neutrons/cm^2 (60 rad for TID),
1 MeV $1 \cdot 10^{13}$ neutrons/cm^2 (400 rad for TID).

Dev2: 20 MeV $3.2 \cdot 10^{10}$ protons/cm^2 (10 krad for TID).
5 MeV $7.8 \cdot 10^{11}$ electrons/cm^2 (20 krad for TID).
5 MeV $1.2 \cdot 10^{12}$ electrons/cm^2 (30 krad for TID).

Dev3: 1 MeV $7 \cdot 10^{13}$ neutrons/cm^2 (3 krad for TID).

Dev4: 20 MeV $2 \cdot 10^{11}$ protons/cm^2 (60 krad for TID).

Dev5: 20 MeV $3 \cdot 10^{11}$ protons/cm^2 (90 krad for TID).
Annealing (100 °C).

Neutron irradiation of the samples was carried out in a two-zone pulsed self-extinguishing fast-neutron reactor [15]. The flux maximum in the reactor spectrum corresponds to neutron energy of 0.2 MeV, while the average neutron energy is 1.25 MeV. The fluence to TID conversion factor for Si is $4 \cdot 10^{-11}$ rad cm^2.

Electron irradiation at room temperature was performed on the linear electron accelerator Linac UELV-10-10-C-70 [16] at the Center of collective use “Physical Measurements Investigations” (CCU PMI) of the Institute of Physical Chemistry and Electrochemistry of the Russian Academy of Science. The flux for 5 MeV electrons is $3 \cdot 10^{10}$ electrons/(cm^2·s).

Proton irradiation was performed on linear accelerator I-2 at the Center of Collective Use “Kamiks” of ITEP [17]. Energy 20 MeV, average flux $1 \cdot 10^{10}$ protons/(cm^2·s). The fluence to ionizing dose conversion factor for Si is $3.9 \cdot 10^{-10}$ rad cm^2.

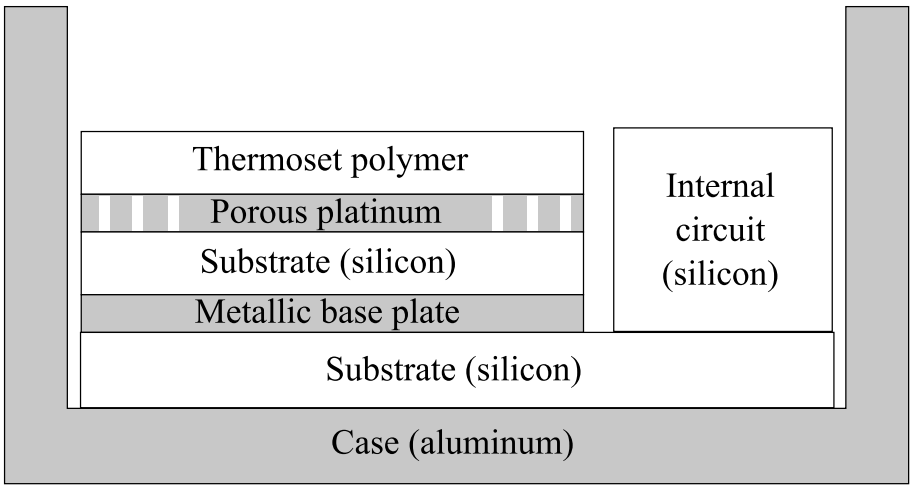

Fig. 2. Structure of RH sensor Honeywell HIH-4000.

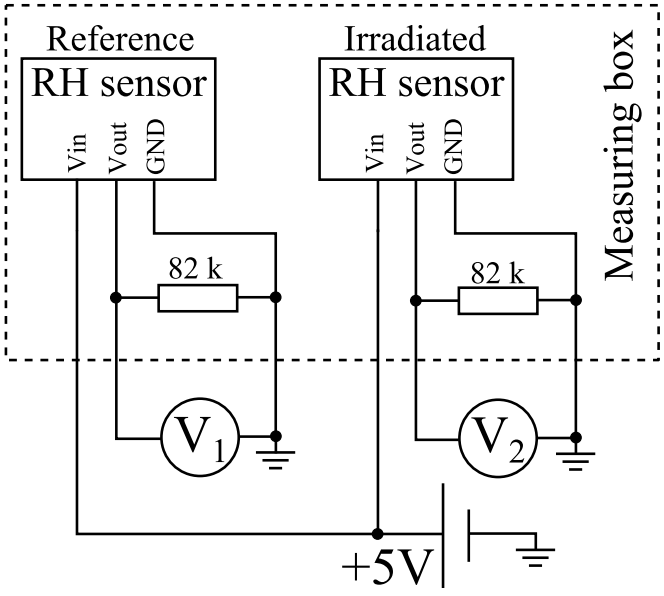

Fig. 3. The measuring circuit.

After every irradiation samples were held for 2 weeks at room temperature. No special high-temperature annealing procedures have not been performed. Irradiated samples were measured and compared with the reference.

Measurements were provided at room temperature. It is not quite the same conditions as in the LHCb experiment: all systems should be cooled down to −5 °C. These RH sensors have temperature drift that can be compensated using correction coefficients [14]. The accuracy and correctness of these coefficients were checked by comparison with Dew-Point meter Vaisala DMT143. Absolute error does not exceed 5% RH.

3. Results and discussion

In this work, samples were tested with neutrons, protons and electrons.

The damage produced by irradiation can be classified into two categories: atomic displacement and charge deposition by ionization. Level of DDD and TID production by charged and neutral particles is very different. Flow of 1 MeV neutrons (fluence $7 \cdot 10^{13}$ particles/cm^2) produces the same DDD as 20 MeV protons (fluence $3 \cdot 10^{11}$ particles/cm^2). But calculated TID for neutrons (3 krad) is much less than for protons (90 krad).

Devices were irradiated by neutrons with different fluences (Dev1 and Dev3), but the output signal does not change significantly. Results of measurements after 1 MeV neutron irradiation (fluence $7 \cdot 10^{13}$ particles/cm^2) are shown on Fig. 4. Straight lines show the sum of absolute and relative errors. Calculated TID (3 krad) is equal to level outside the UT detector after 1 year of LHCb operation.

DDD in Dev3 after neutron irradiation should have the same order of magnitude as Dev4 after 20 MeV proton irradiation. But we found that after neutron irradiation signal output does not change dramatically. At the same time degradation of proton irradiated sample were extremely high (see pic. 6a below). Therefore, we can say that the radiation degradation of the output signal is mainly associated with ionization.

Sample Dev2 was irradiated with 20 MeV protons (absorption TID 10 krad). Results are shown in Fig. 5a. This level of absorption dose is equal to 1-year irradiation in the LHCb experiment (150 cm from beam pipe). After that sample Dev2 was irradiated with 5 MeV electrons (absorption TID 20 krad, 30 in total). The electron mean free path is about 12 mm both in silicon and aluminium [18]. Results are shown in Fig. 5b. It can be seen that output voltage and high-RH sensitivity degrades. Output signal cut off level is 85% with strong distortion in the high-RH part of the curve. Next irradiation with 5 MeV electrons (absorption TID 30 krad, 60 in total) are shown in Fig. 5c. High-RH part of the graph (>40%) is cut off, but the low-RH part does not change dramatically.

The same result can be achieved with protons irradiation. Sample Dev4 was irradiated with 20 MeV protons (absorption TID 60 krad). Results are shown in Fig. 6a. It can be seen that the high-RH part of the graph is cut off, but the low-RH part does not change dramatically (see Fig. 6b). 60 krad is the dose that can be absorbed by the detector after 3 years of LHCb operation.

It can be assumed that degradation of polymer capacitor leads to uniform degradation of sensitivity in all ranges of RH because of capacitance floating. If one of the parts of the internal circuit degrades the output signal changing can be non-uniform. For example, the main radiation effect in silicon-based rectifiers is the increase of leakage current and serial resistance [19–21]. This effect is less noticeable at low forward voltage but precision at high or reverse voltage is dramatically decreased. Limitation of amplifier

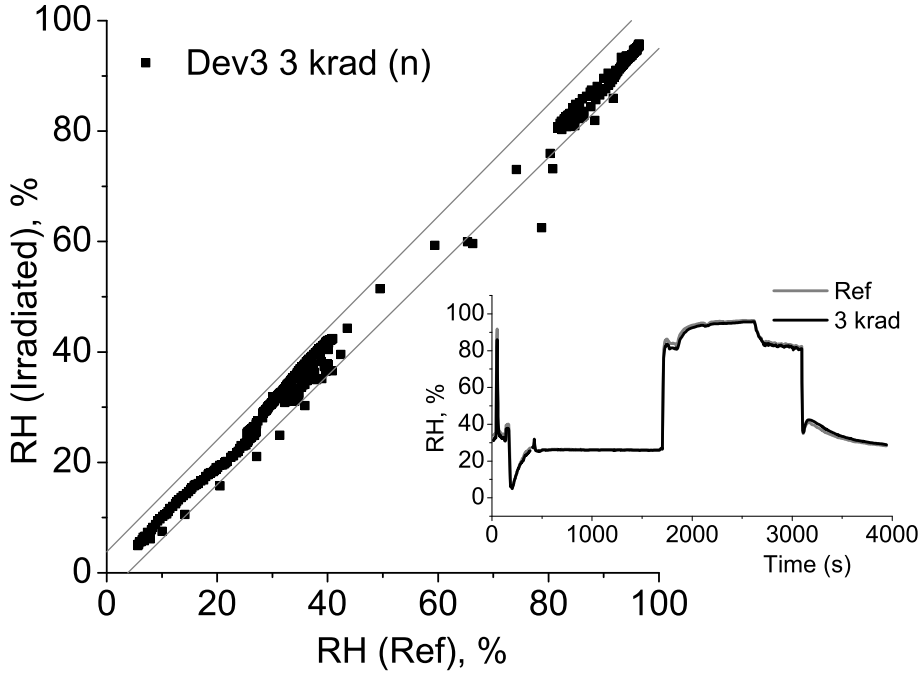

Fig. 4. RH signal after neutron irradiation with absorption dose 3 krad (1 MeV $7{\cdot}10^{13}$ particles/cm^2).

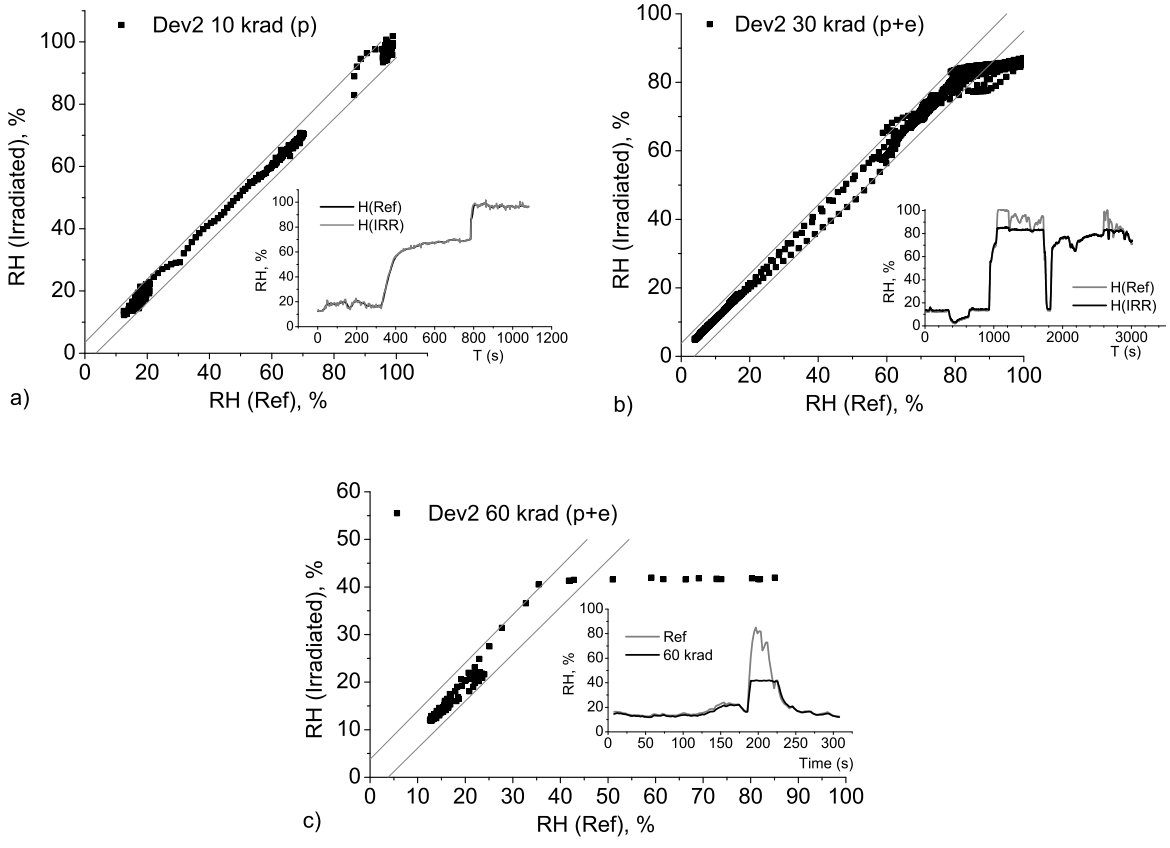

Fig. 5. RH signal after charge particles irradiation:
a – protons with absorption dose 10 krad (20 MeV $3.2{\cdot}10^{10}$ particles/cm^2),
b – (protons +) electrons with absorption dose 20 krad, 30 in total (5 MeV $7.8{\cdot}10^{11}$ particles/cm^2),
c – (protons + electrons +) electrons with absorption dose 30 krad, 60 in total (5 MeV $1.2{\cdot}10^{12}$ particles/cm^2).

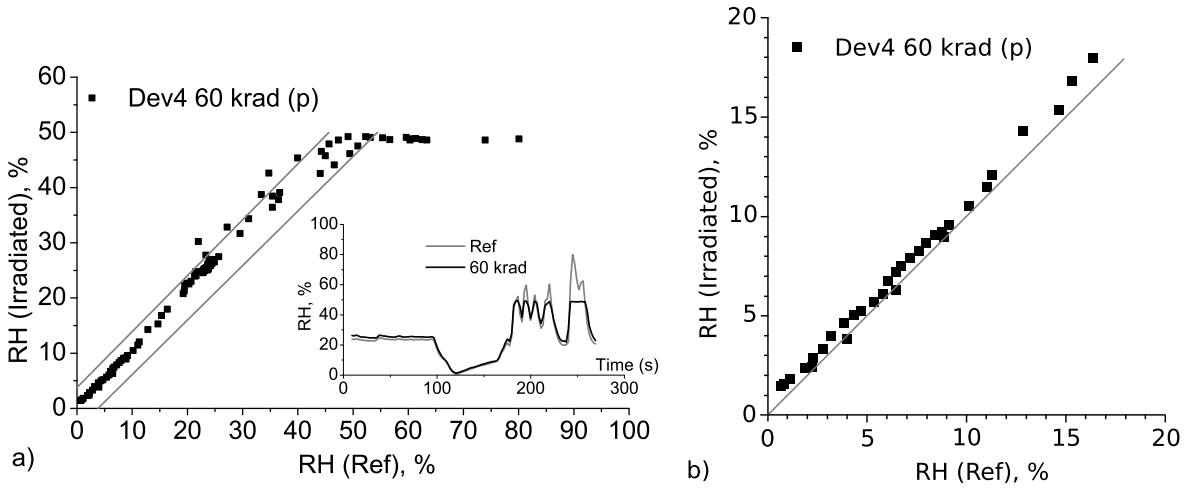

Fig. 6. (a, b). RH signal after proton irradiation with absorption dose 60 krad (20 MeV $2 \cdot 10^{11}$ particles/cm^2).

output level after irradiation associated with current changing was observed before [22,23] and this is presumably the main reason for the discussed effect. In silicon-based devices, radiation effects can be eliminated with annealing. Dev5 was irradiated with electrons up to 90 krad and annealed at 100 °C. After irradiation output voltage does not exceed 50 mV. It is much lower than can be expected (normally output signal should be between 0.8 V for 0% RH and 4 V for 100% RH). Output voltage of irradiated sample corresponded to ambient ~100% RH was measured after annealing, results are shown in Fig. 7. It can be seen that the RH signal cut off level increases after annealing. As radiation degradation of polymer is irreversible [24] this effect confirms the assumption that degradation of RH sensor is mainly determined by silicon electronic part. It can be assumed that the simplest sensor like Honeywell HCH-1000 without any electronics has the best radiation hardness. On the other hand, it is hard to measure small changes in capacitance (0.65 pF/%RH with 330 pF background) with long wires, so the cost and complexity of this solution will increase dramatically. In terms of robustness RH sensor with a simple internal circuit looks like an adequate compromise.

Normally humidity near the LHCb detector should be lower than 10%. The main task for the humidity sensor is to signalize when the RH level will exceed the danger level. For example, if something goes wrong (it might be a problem with nitrogen flow or crack in the box through which ambient air flows inside) humidity can dramatically increase and operation should be stopped. Sensitivity of irradiated sensors in the high-RH range degrades under irradiation as shown on Fig. 8. If environment is not so dry to distinguish the usual RH level from critical it can be unsafe to use this detector. But if the expected RH is low or the RH sensor is quickly replaceable after 1–2 years of operating under irradiation then capacitive humidity sensors can be used in High Energy Physics experiments. Radiation degradation of the RH sensor can be partially reduced with annealing, so irradiated sample can be restored after a few

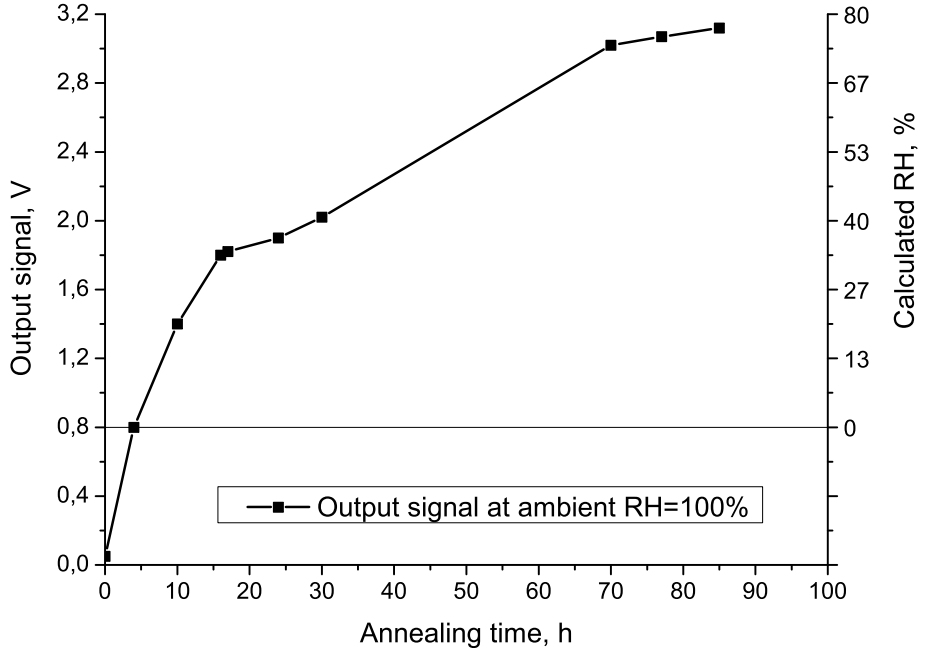

Fig. 7. Output voltage of proton irradiated sample (absorption dose 90 krad, 20 MeV $3 \cdot 10^{11}$ particles/cm^2) corresponded to ambient ~100% RH after annealing.

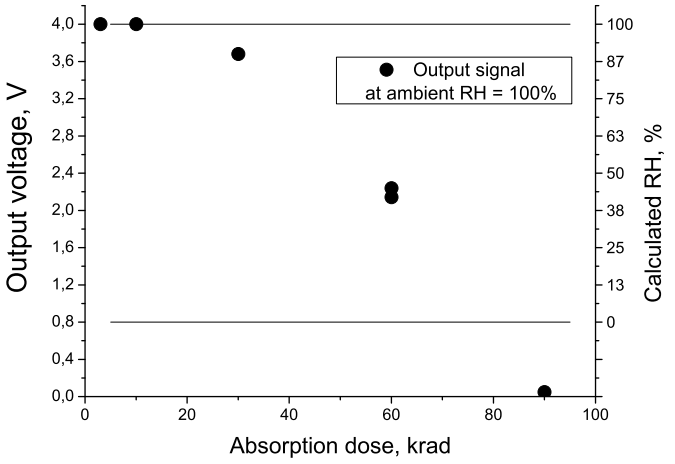

Fig. 8. Relation between the max achievable output signal and absorption dose.

years of operating. The global limit is the degradation of polymer film described in Ref. [10]: output signal slightly increases with fluence: $5.6 \cdot 10^{-15}$% RH/(protons·cm^{-2}).

4. Conclusion

The main radiation effect on the polymer-based capacitive RH sensors is associated with ionization. The most vulnerable part of this sensor is the internal electronic circuit. Irradiation leads to output voltage limit decreasing. High-RH part of output signal degrades, maximum achievable output signal depends on the total ionizing dose. Degradation reduces after annealing.

After 30 krad irradiation by protons and electrons maximum signal of the RH sensor does not exceed 85%. After 60 krad irradiation maximum signal of the RH sensor does not exceed 40%.

Declaration of competing interest

The authors declare that they have no known competing financial interests or personal relationships that could have appeared to influence the work reported in this paper.

References

[1] A.A. Alves Jr., et al., The LHCb detector at the LHC, J. Instrum. 3 (2008) S08005.
[2] A.A. Alves Jr., et al., LHCb detector performance, Int. J. Mod. Phys. 30 (2015), 1530022.
[3] O. Steinkamp, The upstream tracker for the LHCb upgrade, Nucl. Instrum. Methods Phys. Res. 831 (2016) 367–369.
[4] A.L. Buck, New equations for computing vapor pressure and enhancement factor, Am. Meteorol. Soc. 20 (2016) 1527–1532.
[5] D. Rodriguez, et al., Combined effects of humidity and frequency on the dielectric strength of air for VLF applications, in: 2008 Annual Report Conference on Electrical Insulation and Dielectric Phenomena, Quebec, QC, Canada, 2008, pp. 611–614.
[6] LHCb collaboration, LHCb tracker upgrade technical design report, LHCb TDR 15 (21st February 2014).
[7] A. Makovec, et al., Radiation hard polyimide-coated FBG optical sensors for relative humidity monitoring in the CMS experiment at CERN, J. Instrum. 9 (2014) C03040.
[8] H.J. Kim, et al., Fiber-optic humidity sensor system for the monitoring and detection of coolant leakage in nuclear power plants, Nucl. Eng. Technol. 52 (8) (2020) 1689–1696.
[9] A. Kapic, et al., Humidity sensors for high energy Physics applications: a review, IEEE Sensor. J. 20 (2020) 10335–10344.
[10] A. Kapic, et al., Radiation tolerance of capacitive humidity sensor for high-energy Physics applications, IEEE Sens. Lett. 3 (2019) 1–4, 2000604.
[11] W. Petchmaneelumka, P. Phankamnerd, A. Rerkratn, V. Riewruja, Capacitive sensor readout circuit based on sample and hold method, Energy Rep. 8 (2022) 1012–1018.
[12] P. Wu, Z. Xu, C. Meng, et al., The Experiment Study of Effects on ADC Chip against Radiation and Electromagnetic Environment, 12th International Workshop on the Electromagnetic Compatibility of Integrated Circuits, 2019, pp. 207–209.
[13] K. Chen, H. Chen, J. Kierstead, et al., Evaluation of commercial ADC radiation tolerance for accelerator experiments, J. Inst. Met. 10 (2015) P08009.
[14] Datasheet HIH-4000 Series Humidity Sensors, Honeywell, 2010. https://sensing.honeywell.com.
[15] P.P. D'yachenko, O.A. Elovskii, et al., Stand B" reactor-laser system, At. Energy 88 (2000) 352.
[16] Y.S. Pavlov, P.B. Lagov, Magnetic buncher accelerator for radiation hardness research and pulse detector characterization, in: 15th European Conference on Radiation and its Effects on Components and Systems, RADECS), 2015, pp. 1–3.
[17] P.B. Lagov, et al., Proton-irradiation technology for high-frequency high-current silicon welding diode manufacturing, J. Phys.: Conf. Ser. 830 (2017) 12152.
[18] L.A. Aslanov, et al., Nanosilicon stabilized with ligands: effect of high-energy electron beam on luminescent properties, Surf. Interface Anal. (2016) 1–5.
[19] I. Mandi, et al., Measurements with silicon detectors at extreme neutron fluences, J. Instrum. 15 (2020) P11018.
[20] A. Floriduz, J.D. Devine, Radiation Testing of Optical and Semiconductor Components for Radiation-Tolerant LED Luminaires. 2018 18th European Conference on Radiation and its Effects on Components and Systems, RADECS), 2018, pp. 1–8.
[21] A. Uleckas, et al., Investigation of the switching and carrier recombination characteristics in the proton irradiated and thermally annealed Si PIN diodes, Lith. J. Phys. 50 (2) (2010) 225–232.
[22] F.J. Franco, Y. Zong, J. Casas-Cubillos, et al., Neutron effects on short circuit currents of op amps and consequences, IEEE Trans. Nucl. Sci. 52 (5) (2005) 1530–1537.
[23] J.A. Agapito, N.P. Barradas, F.M. Cardeira, et al., Radiation Tests on Commercial Instrumentation Amplifiers, Analog Switches & DAC's. 7th Workshop on Electronics for LHC Experiments, 2001, pp. 117–121.
[24] J. Vohlidal, Polymer degradation: a short review, Chem. Teach. Int. 2 (2020), 20200015.